IEEE Access
Multidisciplinary ⋮ Rapid Review ⋮ Open Access Journal

Received February 17, 2020, accepted February 23, 2020, date of publication February 27, 2020, date of current version March 6, 2020.

Digital Object Identifier 10.1109/ACCESS.2020.2976769

Through-the-Wall Image Reconstruction via Reweighted Total Variation and Prior Information in Radio Tomographic Imaging

QICHANG GUO, YANLEI LI, XINGDONG LIANG, JIAWEI DONG, AND RUICHANG CHENG

National Key Lab of Microwave Imaging Technology, Beijing 100190, China
Aerospace Information Research Institute, Chinese Academy of Sciences, Beijing 100190, China
School of Electronics, Electrical and Communication Engineering, University of Chinese Academy of Sciences, Beijing 100049, China

Corresponding authors: Qichang Guo (guoqc1992@126.com) and Xingdong Liang (xdliang@mail.ie.ac.cn)

ABSTRACT This paper focuses on the application of radio tomographic imaging in through-the-wall image reconstruction. By using the simple wireless communication devices, e.g., Wi-Fi cards, the whole building layout can be reconstructed with only the received signal strength (RSS). For the reconstruction algorithms, the total variation (TV) minimization algorithm has been used to reconstruct the image. However, some false artifacts may exist in the image results due to the inherent defects of the algorithm. The artifacts can be misestimated as wall structures. In this paper, a reweighted total variation and prior information regularization algorithm named as RTV-PIR is proposed to reconstruct the image. This algorithm is based on the TV minimization of the image. And the prior information that the wall is only oriented horizontally or vertically is also considered simultaneously, which is used to keep the wall orientation. To verify the performance of the proposed algorithm, the simulations and experiments based on real data are conducted. It is shown that the RTV-PIR algorithm can get a better result with respect to the root mean square error (RMSE) and the structural similarity (SSIM), in comparison with the state-of-the-art algorithms.

INDEX TERMS Prior information, radio tomographic imaging, through-the-wall, total variation (TV) minimization, Wi-Fi.

I. INTRODUCTION

As a new technology application, through-the-wall radar imaging (TTWRI) has been widely researched [1]–[3]. It can detect the object inside the building by using the ability that the electromagnetic waves can penetrate the dielectric wall, which has vast application prospects ranging from military fields to civilian fields including but not limited to urban street fighting, anti-terrorism and disaster rescue. In the fields of TTWRI, the main purpose of building layout reconstruction aims at obtaining the overall layout information by observation outside the building, which is very important before entering inside the building. The problem of building layout reconstruction has led to more and more attention in recent years [4], [5].

As a whole, it can be divided into two strategies to obtain the building layout image. In the first strategy, the complex radar system is used to obtain the ultra-wideband echo signal reflected from the target. The signal is transmitted from the radar, and reflected from the inner walls back to the radar. The final image is ofen obtained by coherent processing of the received signal in which the phase information is required. In this strategy, the ultra-wideband signal is needed in order to obtain high range resolution. And the high azimuth resolution is obtained by using the synthetic aperture technology [6]. Multiple inputs and multiple outputs (MIMO) also is used to improve the signal-to-clutter (SCR) of the image [7]. In practise, these methods have relatively high resolution. However, the system bandwidth could be large enough. On the other hand, the electromagnetic wave at least penetrates the same wall twice in the propagation, which means the system must have enough transmitting power to ensure the detection distance.

Instead of depending on the complex system and phase information, the simple system, e.g., wireless sensor networks (WSNs) is used to obtain the received signal strength (RSS) in the second strategy. It is very attractive with the advantage of simplexity, low cost and low power

The associate editor coordinating the review of this manuscript and approving it for publication was Gongbo Zhou.

consumtion. In this strategy, the RSS of the system nodes is related to the shadowing loss when the electromagnetic wave signal propagates through the field. Based on RSS, many methods have been proposed in the past few years. Radio tomographic imaging (RTI) was proposed in 2010 [8], which aims at locating the persons' positions by deploying a large number of low-cost wireless sensor network nodes around the targets. In [9], the problem of building layout reconstruction with RTI is considered, which shows that RTI can be used to reconstruct complicated building-like structures. These methods are all based on fixed and distributed network nodes, which reconstruct the spatial loss field (SLF) image with RSS. Armed with two Pioneer 3-AT mobile robots and two directional antennas, the obstacle map is built in [10]. Because of the see-through-the-wall capability, the inner layout map also can be reconstructed. Moreover, based on the mobile platform and two directional antennas, the Rytov model is used to build the obstacle map in [11]. Here the RTI with fix and distributed network nodes is called the fix RTI. The RTI with mobile and two directional antennas is called the mobile RTI. This paper mainly focuses on the mobile RTI.

One main challenge of the RTI still is the reconstruction algorithms. It is well known that the problem of RTI is an ill-posed problem, which means that the measurements are far less than the unknowns. To solve this problem, conventional algorithms mostly utilize some regularization techniques following from a Bayesian approach or eliminating small singular values of the transfer matrix [12], including Tikhonov regularization, truncated singular value decomposition (TSVD) and total variation method. Although these regularization methods can achieve stable results, the image results are quite blurred. In [13], Brian Beck proposed a prior information based regularization method, in which an elliptically-shaped covariance function was used to model the spatial covariances of pixels in the floor plan images. This method can preserve the structure of the floor plan better. But in this regularization method, it must solve the image in the horizontal direction and the image in the vertical direction separately. And the final result is obtained by image fusion. Similar regularization methods are used in [14], [15], but they didn't consider the directions in the spatial covariance of pixels and the structure orientation information was not considered. Generally speaking, the reconstructed wall structure is sparse in the spatial domain or other domain by image transformation, so the compressive sensing (CS) method can be used to reconstruct the image [16]–[19]. Moreover, the total variation (TV) minimization algorithm is used to reconstruct the image and a good image is obtained [20], [21]. The TV minimization algorithm aims at minimizing the total variation of the gradient image in order to get a sparse gradient image. The advantage of TV minimization algorithm than that of regularization method is that the image result can be more sparse and clear. However, the TV minimization algorithm has its inherent defects such as staircase effects [23]. On the other hand, the artifacts may exist in the final results due to the limited-angle measurements and model error.

In this paper, we propose an improved TV minimization algorithm to reconstruct the image, which named as RTV-PIR. In the proposed algorithm, the reweighted total variation (RTV) method is used to set different weights to the TV term in the reconstruction process. At the same time, the prior information about the orientation of the wall structure is also used. The result shows that the proposed method can suppress the artifacts and preserve the wall structure. The main contributions of this paper are:

- Summarizing the through-the-wall mobile RTI problem. The current shadowing model is presented and the weight values are derived using the Rytov linear approximation.
- Proposing an RTV-PIR algorithm to reconstruct the SLF image. The TV minimization algorithm is improved by combining the reweighted total variation (RTV) minimization and the prior information of the image structure orientation.
- Conducting a real through-the-wall experiment to verify the effectiveness of the RTV-PIR algorithm. The results show the quality of the image structure is improved in comparison with the state-of-the-art algorithms.

The rest of this paper is organized as follows: In section II, the problem of through-the-wall mobile RTI is summarized briefly. In section III, we introduce the proposed RTV-PIR algorithm in details. The numerical simulations and real experiment are conducted and discussed in section IV. Finally, the conclusions are drawn in section V.

II. THROUGH-THE-WALL MOBLIE RTI

In general, an area of interest D is considered, which is shown in Figure 1. The transmitting antenna and receiving antenna are placed on two mobile platforms outside the building, aiming at getting information about the internal structure. The transceiver platform scans in different directions with step size d, according to the principle of computerized tomography (CT). Figure 1 shows the scanning schematic at 0^o, 45^o, 90^o and 135^o. The direction is defined as the angle between the moving line and the positive direction of the x axis. The positions of the transmitting antenna and receiving antenna are (t_n, r_n). The directional antennas are used in order to reduce the environmental impact, e.g., multipath. To guarantee low observation error, the main lobe of the transmitting antenna is always aligned with the main lobe of the receiving antenna. At every location, the wireless signal is transmitted by the transmitter, and the RSS at every position of the receiver is measured. M RSS measurements are obtained in total, which are used to reconstruct the SLF image.

Due to the effect of the enviorment, the relation between the RSS measurements and the SLF is nonlinear [24]. But the nonlinear problem is difficult to deal with in practice. Thus, some linear models are considered to represent the relation approximately. In [8], Wilson and Patwari proposed the normalized elliptical model to express the shadowing effect of the wireless signal caused by the obstacles. In the

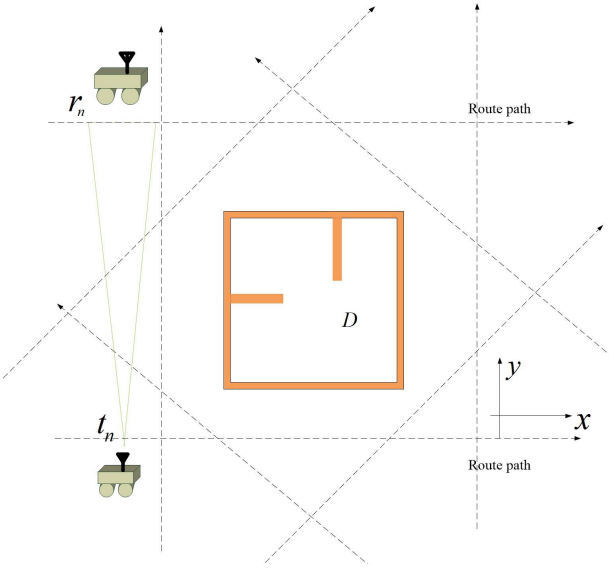

FIGURE 1. Through-the-wall mobile RTI scheme.

model, the area of interest is discretized into a series of pixels. By making different weights to different pixels, the shadowing effect can be mathematically expressed in the following form

$$P_s(t_n, r_n) = \sum_{j=1}^{N} w_{nj} g(j) + n \tag{1}$$

In the above equation, $P_s(t_n, r_n)$ is the shadowing attenuation of the wireless signal when the transceiver is at position (t_n, r_n). It can be obtained with the RSS measurement by removing the effect of path loss and transmitting/receiving antenna gains. n is the noise denoting the model error. $g(j)$ denotes the SLF in the pixel j and w_{nj} is the weight of pixel j to represent the attenuation effect to the wireless signal transmission, which is

$$w_{nj} = \frac{1}{\sqrt{|r_n - t_n|}} \begin{cases} 1, & |r_j - t_n| + |r_j - r_n| < |r_n - t_n| + \lambda \\ 0, & others \end{cases} \tag{2}$$

where $|r_n - t_n|$ is the length between the transmitter and receiver. $|r_j - t_n|$ and $|r_j - r_n|$ denote the euclidean distance of the transceiver and piexl j respectively. λ is the parameter to determine the size of ellipse area [8]. In the normalized elliptical model, the physical basis behind it is that the first Fresnel zone has an ellipsoidal shape and the most engry is limited into the internal ellipse when transmission. But it has no physical justification that the weights are all the same inside the ellipse. It is generally known that different pixels should have different weights due to the the difference of distance. How to model the difference has been a hot topic in recent years. The most intuitive feeling is that the longer the distance between the transceiver and the pixel is, the smaller the weight is. And based on this concept, some modified elliptical models have been proposed [25], [26]. However, they are all empirical models lacking of physical foundation. In this paper, the Rytov linear model is used to represent the weights inside the ellipse, which has more clear physical justification and is more precise in practise.

In the Rytov model, the total electric field at the receiver can be expressed as [24]

$$E_t(r_n, t_n) = e^{\phi(r_n, t_n)} = e^{\phi_i + \phi_s} \tag{3}$$

where ϕ_i is the complex incident field phase. ϕ_s is the complex scattering field phase. (3) can be rewritten in the following form

$$\begin{aligned} E_t(r_n, t_n) &= E_i(r_n, t_n) e^{\phi_s(r_n, t_n)} \\ \phi_s(r_n, t_n) &= \frac{k_0^2}{E_i(r_n, t_n)} \iint_D g(r_n, r') E_i(r', t_n) O(r') dr' \end{aligned} \tag{4}$$

where k_0 is the propagation constant in free space. $g(r', t_n)$ is the Green's function with the explicit expression

$$g(r', r_n) = \frac{j}{4} H_0^1(k_0 |r - r_n|) \tag{5}$$

$H_0^1(k_0|r' - r_n|)$ is the Hankel function of the first kind and zero order. $E_i(r_n, t_n)$ is the incident field at the location r_n. $O(r')$ is the relative permittivity in the area of interest which is the unkowns and is reconstructed with RSS measurements. More information about the Rytov model can be found in [24], [27]. The RSS can be obtained by (4) and that is

$$P_t(r_n, t_n) = |E_t(r_n, t_n)|^2 = |E_i(r_n, t_n)|^2 e^{2Re[\phi_s(t_n, r_n)]} \tag{6}$$

The shadowing attenuation in dB can be obtained by removing the effect of path loss and gains of the transmitter and the receiver, which is

$$P_t(r_n, t_n) = P_t(r_n, t_n) - P_0(r_n, t_n) = (20 \log 10) Re[\phi_s(r_n, t_n)] \tag{7}$$

where the effects of the path loss and the transceiver gains are included in $P_0(r_n, t_n)$. So the weight of the pixel r' can be represented as

$$w_{nr'} = (20 log_{10} e) Re[\frac{k_0^2}{E_i(r_n, t_n)} g(r_n, r') E_i(r', t_n)] \tag{8}$$

The weight is obtained approximately by discretting (7) and considering that the imaginary part of $O(r')$ is much smaller than the real part [11]. Next, (8) is simplified by utilizing the relation between the incident field and Green's function

$$\begin{aligned} E_i(r_n, t_n) &= j\omega G(r_n, t_n) g(r_n, t_n) \\ E_i(r', t_n) &= j\omega G(r', t_n) g(r', t_n) \end{aligned} \tag{9}$$

ω is the angular frequency and equals $2\pi f_0$, where f_0 is $2.437 GHz$ in our experiments. $G(r_n, t_n)$ and $G(r', t_n)$ are the gains of the transmitting antenna at the location r_n and r'. In the elliptical area, these two values are approximately equal

due to the reason that only the pixels near the LOS area are considered. So the weight of the pixel r' can be simplified to

$$\begin{aligned} w_{nr'} &= (20log_{10}e)Re[\frac{k_0^2 g(r_n, r')g(r', t_n)}{g(r_n, t_n)}] \\ &= (20log_{10}e)Re[\frac{jk_0^2 H_0^1(k_0|r_n - r'|)H_0^1(k_0|r' - t_n|)}{4H_0^1(k_0|r_n - t_n|)}] \end{aligned} \tag{10}$$

Finally, the weight model can be written as

$$w_{nr'} = (20\log_{10}e)\begin{cases} t, & |r' - t_n| + |r' - r_n| < |r_n - t_n| + \lambda \\ 0, & others \end{cases} \tag{11}$$

where $t = Re[\frac{jk_0^2 H_0^1(k_0|r_n - r'|)H_0^1(k_0|r' - t_n|)}{4H_0^1(k_0|r_n - t_n|)}]$. The next step is to reconstruct the SLF image with RSS measurements. Assuming that the image is discretized into N pixels and M RSS measurements are obtained in total, the matrix form of the shadowing attenuation can be written as

$$P_s = WO + N \tag{12}$$

where the vector of the shadowing obtained by the RSS $P_s = [P_s(t_1, r_1), P_s(t_2, r_2), \ldots, P_s(t_M, r_M)]^T \in R^M$. The weighting model matrix $W = [w_1, w_2, \ldots, w_M]^T \in R^{M \times N}$, $w_l = [w_{l1}, w_{l2}, \ldots, w_{lN}]^T \in R^N$. The noise vector $N = [N_1, N_2, \ldots, N_M]^T$. The final SLF image can be obtained by solving (12).

III. RTV-PIR ALGORITHM

A. THE RTV-PIR MODEL

Since W is under-determined, the problem of through-the-wall mobile RTI is an ill-posed problem. To correct this, conventional methods mostly utilize Tikhonov regularization, which adds an additional norm constraint on the SLF image such that the poor condition can be compensated. The Tikhonov approach only considers the correlation property in the SLF image. The reconstruction result is usually blurred [8], [9]. Due to the reason that the wall structures are sparse in the whole SLF image, the compressive sensing (CS) methods have been used in the image reconstruction [17]–[19]. Moreover, cosidering the greater sparsity of the image in the gradient domain, TV minimization model [11] has been used to reconstruct the SLF map in through-the-wall image reconstruction. The TV minimization method solves the following cost function

$$\min_O(\frac{\mu}{2}\|WO - P_s\|_2^2 + \|D_x O\|_1 + \left\|D_y O\right\|_1) \tag{13}$$

where $D_x O$ and $D_y O$ are the vectors arranged by the horizontal and vertical gradient image, which are defined as

$$\begin{aligned} [D_x O]_{i,j} &= \begin{cases} O_{i,j+1} - O_{i,j}, & j \neq m \\ O_{i,1} - O_{i,m}, & j = m \end{cases} \\ [D_y O]_{i,j} &= \begin{cases} O_{i+1,j} - O_{i,j}, & i \neq n \\ O_{1,j} - O_{n,j}, & i = n \end{cases} \end{aligned} \tag{14}$$

m and n denote the length and width of image respectively. The above optimization problem in (13) can be solved effectively by the typical TVAL3 algorithm (TV Minimization by Augmented Lagrangian and Alternating Direction Algorithms) [29].

However, the original TV minimization algorithm suffers from some inherent defects such as the staircase artifact [23], which limits the reconstruction quality. To solve the problem, the reweighted total variation (RTV) model has been proposed to preserve the edge of image by reweighting the TV term in the reconstruction [30], which is given as

$$\min_O(\frac{\mu}{2}\|WO - P_s\|_2^2 + \|g_x \odot D_x O\|_1 + \left\|g_y \odot D_y O\right\|_1) \tag{15}$$

where $\odot$ is the element-to-element product. g_x and g_y are the vectors of the weight to reweight the TV term in the reconstruction. The concept of the reweighting is that the TV term is reweighted by detecting the values of horizontal and vertical gradient images in the iteration process, which is

$$\begin{aligned} g_x(i,j) &= \begin{cases} 1, & |D_x O(i,j)| > \tau \\ 0, & others \end{cases} \\ g_y(i,j) &= \begin{cases} 1, & |D_y O(i,j)| > \tau \\ 0, & others \end{cases} \end{aligned} \tag{16}$$

where τ is the threshold value to determine the weights. When the weights are assigned 0, the pixels have large jumps and they do not contribute anything to the TV [28]. By this way, TV can focus on other pixels and the staircase artifacts can be suppressed.

The RTV model considers the edge information in the reconstruction and can suppress the staircase artifact to a certain extent. But it still doesn't perform well with the limited-angle measurements and noise. The artifacts may exist in the results and the structure can not be kept clear. As we can see, the RTV model doesn't consider the prior information of the image. Since the wall structure is only oriented horizontally and vertically, the prior information about the wall orientation can be used in the reconstruction. So in this paper, we propose a new algorithm named RTV-PIR which combines the RTV and the prior information of the orientation together to improve the quality of reconstruction. The objective function can be written as

$$\begin{aligned} \min_O(\frac{\mu}{2}\|WO - P_s\|_2^2 + \|g_x \odot D_x O\|_1 + \left\|g_y \odot D_y O\right\|_1 \\ +\alpha\|QO\|_2^2) \end{aligned} \tag{17}$$

where the last item is taken from L_2 norm regularization to penalize the energy in QO, for some specified linear operator Q. α is the regularization parameter to control the penalty term's smoothing effect on the solution. It has been observed that the regularization can be related to the Bayesian covariance via

$$\|QO\|_2^2 = O^T C^{-1} O \tag{18}$$

where C^{-1} denotes the inverse of spatial covariance matrix of the image. Here the expression proposed in [13] is used, which is

$$C(i,j) = e^{-\sqrt{(\frac{d_x(i,j)}{\kappa_x})^2+(\frac{d_y(i,j)}{\kappa_y})^2}} \tag{19}$$

$d_x(i,j)$ and $d_y(i,j)$ are the horizontal and vertical distances between the pixel i and the pixel j. κ_x and κ_y are the parameters to control the rate at which C falls off in the x and y directions independently. It can be seen that by setting $\kappa_x \gg \kappa_y$, the spatial covariance becomes highly oriented in the x direction. This is set when the current pixel is a part of the horizontal wall structure. If the information of the wall orientation in every pixel is known, the κ_x and κ_y of every pixel can be determined. But the directions of wall structure in every pixel is unknowable before reconstruction. So most methods in the literature set equal value to κ_x and κ_y, which means the prior information of the wall orientation is not used. Fortunately, the edge can be detected with g_x and g_y in the iteration process. The values of κ_x and κ_y can be determined with the detected edge information. In particular, the values of every pixel are assigned as

$$(\kappa_x(i,j), \kappa_y(i,j)) = \begin{cases} (k_1, k_2), & g_x(i,j) > g_y(i,j) \\ (k_2, k_1), & g_x(i,j) < g_y(i,j) \\ (k_2, k_2), & g_x(i,j) = g_y(i,j) \end{cases} \tag{20}$$

where $k_2 \gg k_1$. It can be seen that when $g_x > g_y$, the current pixel is a part of the vertical wall structure. When $g_x < g_y$, the current pixel is a part of the horizontal wall structure. When $g_x = g_y$, that means the value of g_x and g_y is 0 or 1. If the value is 0, it is shown that the current pixel is not wall structure. If the value is 1, it is shown that the current pixel is a part of the wall structure whose orientation is slopping. But the prior information shows that there is no sloping wall structure in the image, which means that the detected sloping wall structure is an artifact. So the κ_x and κ_y of the current pixel is set k_2. By this way, the wall structure can be preserved in the reconstruction.

B. THE OPTIMIZATION PROCEDURE

To minimize the objective function in (17), here we develop an algorithm using the alternating direction method of multipliers (ADMM) [31]. Specifically, by introducing auxiliary variables, (17) can be rewritten as

$$\begin{aligned} &\min_O(\frac{\mu}{2}\|WO - P_s\|_2^2 + \|g_x \odot U_x\|_1 + \|g_y \odot U_y\|_1 \\ &\qquad +\alpha\|QO\|_2^2) \\ &s.t. U_x = D_x O, U_y = D_y O \end{aligned} \tag{21}$$

The augmented Lagrangian function of the above optimization can be reconstructed as

$$\begin{aligned} &L(O, U_x, U_y) \\ &= \frac{\mu}{2}\|WO - P_s\|_2^2 + \|g_x \odot U_x\|_1 + \|g_y \odot U_y\|_1 \\ &\quad - {\lambda_x}^T(U_x - D_x O) + \frac{\beta_x}{2}\|U_x - D_x O\|_2^2 \\ &\quad - {\lambda_y}^T(U_y - D_y O) + \frac{\beta_y}{2}\|U_y - D_y O\|_2^2 + \alpha\|QO\|_2^2 \end{aligned} \tag{22}$$

where λ_x and λ_y are the Lagrangian multipliers vectors, and β_x and β_y are the parameters to control the weight. According to the framework of ADMM, the optimization problem with respect to each variable in (22) can be solved by the following optimization subproblems.

1) U_x and U_x Subproblems: The optimization subproblem with respect to U_r (r can be either x or y) can be rewritten as

$$\begin{aligned} &\min_{U_r} L(U_r) \\ &= (\|g_r \odot U_r\|_1 - {\lambda_r}^T(U_r - D_r O) + \frac{\beta_r}{2}\|U_r - D_r O\|_2^2) \end{aligned} \tag{23}$$

which U_r can be solved by the soft-threshold shrinkage operator as follows:

$$U_r = sth(D_r O + \frac{\lambda_r}{\beta_r}, \frac{g_r}{\beta_r}) \tag{24}$$

where $sth(x,\tau) = sgn(x)max(|x| - \tau, 0)$.

2) O Subproblem: The minimization with respect to O is given as

$$\begin{aligned} &\min_O L(O) \\ &= (\frac{\mu}{2}\|WO - P_s\|_2^2 - {\lambda_x}^T(U_x - D_x O) + \frac{\beta_x}{2}\|U_x - D_x O\|_2^2 \\ &\quad -{\lambda_y}^T(U_y - D_y O) + \frac{\beta_y}{2}\|U_y - D_y O\|_2^2) + \alpha\|QO\|_2^2 \end{aligned} \tag{25}$$

which the minimization of (25) can be solved by the off-the-shelf techniques such as the conjugate gradient method and O can be obtained by iteration.

3) Updating Multipliers Vectors: According to the framework of ADMM, the multipliers λ_x and λ_y are updated by the following formulas:

$$\begin{aligned} \lambda_x &= \lambda_x - \beta_x(U_x - D_x O) \\ \lambda_y &= \lambda_y - \beta_y(U_y - D_y O) \end{aligned} \tag{26}$$

The previous reconstructed image is used to estimate the g_x, g_y, κ_x and κ_y. In addition, we update the above four parameters after K iterations. The proposed RTV-PIR algorithm can be summarized in Algorithm 1.

IV. VALIDATION

In this section, we will describe the performance of the proposed algorithm RTV-PIR. The simulations and experiments based on real data are conducted. The performance of RTV-PIR is discussed and the algorithm is compared with the typical TV minimization algorithms to demonstrate the effectiveness of the proposed algorithm.

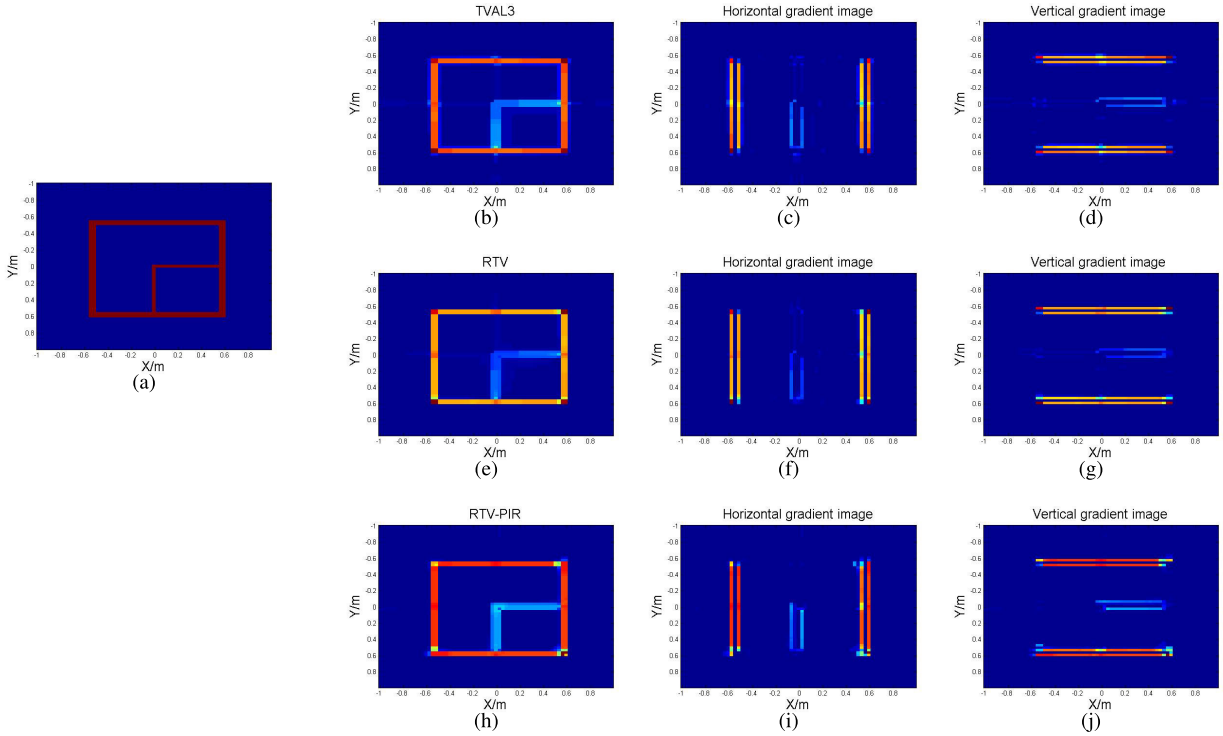

FIGURE 2. The original image and the reconstructed results. (a) The original image. (b) The reconstructed result with TVAL3. (c)-(d) The reconstructed horizontal and vertical gradient image with TVAL3. (e) The reconstructed result with RTV. (f) - (g) The reconstructed horizontal and vertical gradient image with RTV. (h) The reconstructed result with RTV-PIR. (i) -(j) The reconstructed horizontal and vertical gradient image with RTV-PIR.

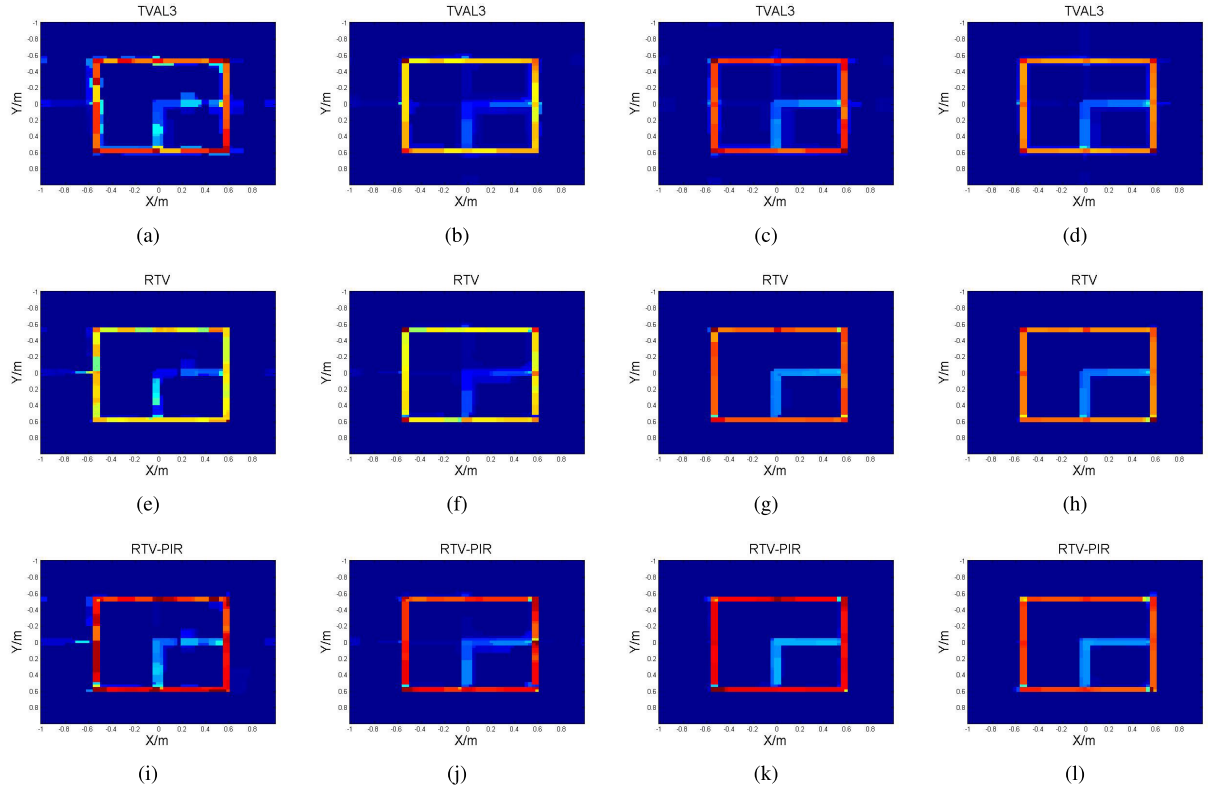

FIGURE 3. The reconstructed results with SNRs from 0 dB to 15 dB. (a)-(d) The results of TVAL3. (e)-(h) The results of RTV. (i)-(l) The results of RTV-PIR.

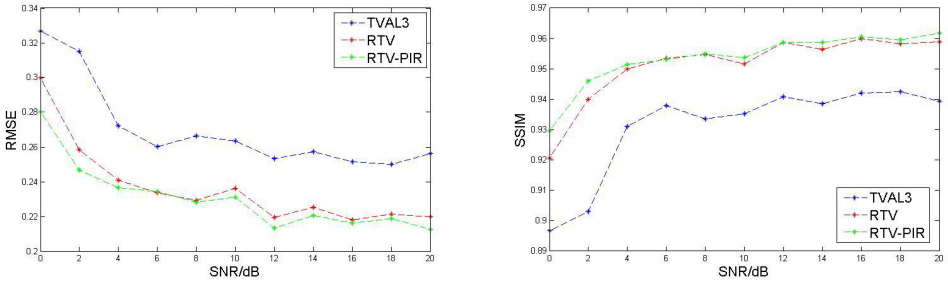

(a) (b)

FIGURE 4. The RMSE and SSIM with different SNRs.

(a) (b) (c)

FIGURE 5. (a) The block diagram of the experimental system. (b) The experimental environment. (c) The experimental target.

Algorithm 1 RTV-PIR

Input: The RSS measurement vector P_s, the weighting model matrix W, the algorithm parameters α, μ, k_1, k_2, g_x, g_y, κ_x, κ_y, λ_x, λ_y, β_x and β_y.

Initialization: $O = 0$, $g_x = g_y = 1$, $\lambda_x = \lambda_y = 0$, the other variables are initialized by experience.

While $t < nMax$ and $\frac{\|O^{t+1}-O^t\|_2^2}{\|O^t\|_2^2} > tol$ **do**

  for $i = 1$ to K **do**

    Solving the subproblem in (23);

    Solving the subproblem in (25);

    Updating the multipliers in (26);

  end for

  Updating g_x and g_y in (16) with a threshold τ.

  Updating κ_x and κ_y in (20).

  $t = t + 1$.

end while

Output: The reconstructed O.

A. NUMERICAL EVALUATION INDEX

Before the introduction of the numerical simulations and experimental results, the numerical evaluation indexes are presented in order to quantitatively analyze and compare the performance of the proposed algorithm. In this paper, the root mean square error (RMSE) and the structural similarity (SSIM) are used to evalute the reconstructed quality. The RMSE is defined as follows:

$$RMSE = \sqrt{\frac{\sum_{i=1}^{N}(x_{i_{rec}} - x_{i_{ori}})^2}{N}} \tag{27}$$

where N is the total number of pixels in the image, $x_{i_{rec}}$ and $x_{i_{ori}}$ represent the i-th pixel values of the reconstructed image and the original image, respectively.

The SSIM is aimed at comparing the structural similarity between the reconstructed image and the original image [30]. The definition of SSIM is as follows:

$$SSIM = \frac{(2\mu_A\mu_B + c_1)(2\sigma_{AB} + c_2)}{(\mu_A^2 + \mu_B^2 + c1)(\sigma_A^2 + \sigma_B^2 + c_2)} \tag{28}$$

where μ_A and μ_B are the average pixel values of the reconstruction image and the original image, respectively. σ_A and σ_B are the variances of the reconstruction image and the original image, respectively. σ_{AB} is the covariance between the reconstruction image and the original image. c_1 and c_2 are the constants used to stabilize the formula; and $c_1 = (k_1L)^2$, $c_2 = (k_2L)^2$, L is the dynamic range of pixel values. The SSIM value is from 0 to 1, if the value is closer to 1, the reconstructed image has more similar structure to the original image. We will calculate the SSIM between the reconstructed image and the original image with the proposed algorithm later.

B. NUMERICAL SIMULATIONS

The original image in the simulations is shown in Figure 2(a). The reconstructed target is a square room whose exterior wall and interior wall are only oriented horizontally or vertically. Four different scanning directions of 0^o, 45^o, 90^o and 135^o are involved in the simulations and the Rytov linear model mentioned before is used to obtain the RSS values. Some important parameters are listed in Table 1. The common parameters among the three algorithms are set the same.

TABLE 1. Some important parameters in the simulations.

Parameter	Value
The length of image	2m
The length of exterior wal	1.12m
The length of interior wal	0.5m
The length of pixel	0.03m
The thickness of exterior wall	0.06m
The thickmess of interior wall	0.03m
μ	2^{10}
a	1
k_1	0.1
k_2	0.01
β_r	2^5
K	30

We use RTV-PIR to reconstruct the image in the simulations. At the same time, in order to compare the performance of RTV-PIR, the typical TV minimization algorithms including TVAL3 and RTV are also used to reconstruct the image. The reconstructed results with these algorithms are shown in Figure 2. It can be seen that some artifacts exist in the result reconstructed with TVAL3. And the staircase are distributed on both sides of the wall structure. In the results of RTV, the staircase is suppressed to a certain extent. However, the artifacts still exist. In the reconstructed result of RTV-PIR, by contrast, the artifacts and staircases are suppressed evidently and the structure is kept clearer. Further, the gradient images reconstructed with these algorithms are also shown in Figure 2, which can be seen that the gradient images with RTV-PIR are clearer and the wall structure is more precise.

Figure 3 shows the reconstruction performance of RTV-PIR with different noise levels. The SNRs are set manually 0 dB to 15 dB with a step of 5 dB. The results are reconstructed with these three algorithms separately. It is shown that the construction quality tends to improve when SNR increases. The reconstruction quality of RTV-PIR is obviously better than that of the other ones. Moreover, the RMSE and SSIM with different SNRs are shown in Figure 4, which validate that the RTV-PIR can obtain higher SSIM and smaller RMSE within the noise level range.

C. EXPERIMENTAL RESULTS AND DISCUSSION

To verify the performance of the proposed algorithm in practice, a real experiment is carried out. The system diagram of our experiment is shown in Figure 6(a), which including a wireless router, two directional antennas, a Raspberry Pi and a remote PC. The Wi-Fi signal is generated by the common wireless router. The transmitting antenna is connected to the wireless router to transmit wireless signals. In order to suppress clutter, the directional grid antenna is used, which has a 19 dBi gain with 21-degree horizontal and 17-degree vertical beamwidth and operates at 2.4GHz ISM frequency band. The Raspberry Pi is utilized to measure the RSS at every receiver location. The data is transferred to the PC in the process. The experimental target is shown in Figure 6(b) and Figure 6(c), which is a wooden structure with side length 1m×1m, exterior wall thickness 0.06m and interior wall

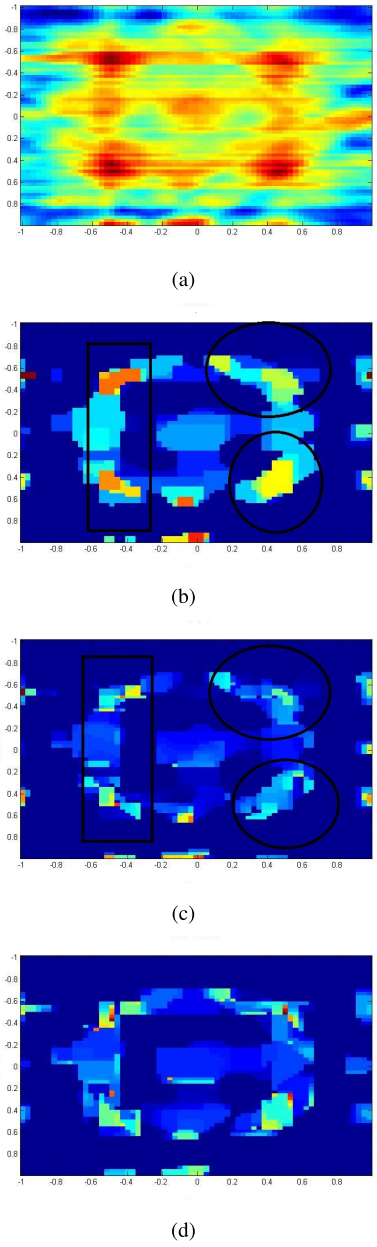

FIGURE 6. (a) The reconstructed image of the regularization method in [10]. (b) The reconstructed image of TVAL3 method. (c) The reconstructed image of RTV method. (d) The reconstructed image of the proposed RTV-PIR method.

thickness 0.03m. In the experimental process, in order to get enough information about the structure, four different scanning directions of 0^o,45^o,90^o and 135^o are conducted. We move the antennas at every scanning directions with step size 0.03m and measurement the RSS at every location.

Next, we reconstruct the image with the RSS measurements using the above algorithms. In our proposed RTV-PIR algorithm, we utilize the prior information that there are only horizontal and vertical wall structures. And we use the variable parameters κ_x and κ_y to preserve the structure in the iterative process, here k_2 and k_1 are set 0.2 and 0.02 empirically. At the same time, the improved regularization method

proposed in [15] recently is also used to reconstruct the image to compare the performance of these algorithms. The results are shown in Figure 6. The reconstructed result of the regularization method in [15] is shown in Figure 6(a), which can be seen that the result is very blurred and the wall structure can't be kept well. Figure 6(b) shows the result reconstructed with the TVAL3 method. The result is clearer than the one in Figure 6(a). However, as mentioned before, the staircase exists in the result and there are sloping wall structures as shown in Figure 6(b). The quality can be improved in the result of RTV, which can be seen as shown in Figure 6(c). However, there still are sloping wall structures as shown in the ellipse region of Figure 6(c). The prior information about the structure orientations is not used in the reconstruction of RTV. Considering the prior information about the wall structure orientations, the result of the proposed RTV-PIR method is shown in Figure 6(d). It can be seen that the result is more clearer and the solping wall structure is suppressed well so that the whole image is more precise.

V. CONCLUSION

In this paper, the problem of through-the-wall radio tomographic imaging is considered. We mainly focus on the reconstruction algorithm. Due to the inherent defects of the TV minimization algorithm, some false artifacts may exist in the image results. To address this, an RTV-PIR reconstruction algorithm is proposed in this paper. The RTV-PIR algorithm combines the reweighted total variation and prior information regularization together, which can suppress the artifacts and keep the wall structure orientations better in the result. In particular, the simulations and real experiment are conducted to validate the effectiveness of the proposed algorithm. It is shown that the RTV-PIP algorithm can obtain better reconstruction results with respect to RMSE and SSIM, and the wall structure orientations can be preserved more accurate. For the future work, we will mainly focus on more accurate inversion in through-the-wall radio tomographic imaging such as three-dimensional layout reconstruction.

REFERENCES

[1] E. J. Baranoski, "Through-wall imaging: Historical perspective and future directions," *J. Franklin Inst.*, vol. 345, no. 6, pp. 556–569, Sep. 2008.

[2] A. Al-Shamma'a and J. P. Edgcombe, "Latest advances in through-wall radar sensing for security applications," *Sensor Rev.*, vol. 28, no. 3, pp. 205–211, 2008.

[3] S. Guo, G. Cui, L. Kong, and X. Yang, "An imaging dictionary based multipath suppression algorithm for through-wall radar imaging," *IEEE Trans. Aerosp. Electron. Syst.*, vol. 54, no. 1, pp. 269–283, Feb. 2018.

[4] B. Yektakhah and K. Sarabandi, "All-directions Through-the-Wall imaging using a small number of moving omnidirectional bi-static FMCW transceivers," *IEEE Trans. Geosci. Remote Sens.*, vol. 57, no. 5, pp. 2618–2627, May 2019.

[5] Y. Song, J. Hu, N. Chu, T. Jin, J. Zhang, and Z. Zhou, "Building layout reconstruction in concealed human target sensing via UWB MIMO through-wall imaging radar," *IEEE Geosci. Remote Sens. Lett.*, vol. 15, no. 8, pp. 1199–1203, Aug. 2018.

[6] T. Dogaru and C. Le, "SAR images of rooms and buildings based on FDTD computer models," *IEEE Trans. Geosci. Remote Sens.*, vol. 47, no. 5, pp. 1388–1401, May 2009.

[7] Y. Jia, G. Cui, L. Kong, and X. Yang, "Multichannel and multiview imaging approach to building layout determination of through-wall radar," *IEEE Geosci. Remote Sens. Lett.*, vol. 11, no. 5, pp. 970–974, May 2014.

[8] J. Wilson and N. Patwari, "Radio tomographic imaging with wireless networks," *IEEE Trans. Mobile Comput.*, vol. 9, no. 5, pp. 621–632, May 2010.

[9] B. R. Hamilton, X. Ma, R. J. Baxley, and S. M. Matechik, "Propagation modeling for radio frequency tomography in wireless networks," *IEEE J. Sel. Topics Signal Process.*, vol. 8, no. 1, pp. 55–65, Feb. 2014.

[10] Y. Mostofi, "Compressive cooperative sensing and mapping in mobile networks," *IEEE Trans. Mobile Comput.*, vol. 10, no. 12, pp. 1769–1784, Dec. 2011.

[11] S. Depatla, L. Buckland, and Y. Mostofi, "X-ray vision with only WiFi power measurements using rytov wave models," *IEEE Trans. Veh. Technol.*, vol. 64, no. 4, pp. 1376–1387, Apr. 2015.

[12] C.-Y. Chiu and D. Dujovne, "Experimental characterization of radio tomographic imaging using Tikhonov's regularization," in *Proc. IEEE Biennial Congr. Argentina (ARGENCON)*, Jun. 2014, pp. 468–472.

[13] B. Beck, R. Baxley, and X. Ma, "Regularization techniques for floor plan estimation in radio tomographic imaging," in *Proc. IEEE Global Conf. Signal Inf. Process.*, Dec. 2013, pp. 177–180.

[14] B. Beck, X. Ma, and R. Baxley, "Ultrawideband tomographic imaging in uncalibrated networks," *IEEE Trans. Wireless Commun.*, vol. 15, no. 9, pp. 6474–6486, Sep. 2016.

[15] S. Xu, H. Liu, F. Gao, and S. Chen, "Experimental verification: Enabling obstacle mapping based on radio tomographic imaging," in *Proc. IEEE 88th Veh. Technol. Conf. (VTC-Fall)*, Chicago, IL, USA, Aug. 2018, pp. 1–5.

[16] M. Bocca, A. Luong, N. Patwari, and T. Schmid, "Dial it in: Rotating RF sensors to enhance radio tomography," in *Proc. 11th Annu. IEEE Int. Conf. Sens., Commun., Netw. (SECON)*, Jun. 2014, pp. 600–608.

[17] K. Huang, S. Tan, Y. Luo, X. Guo, and G. Wang, "Enhanced radio tomographic imaging with heterogeneous Bayesian compressive sensing," *Pervas. Mobile Comput.*, vol. 40, pp. 450–463, Sep. 2017.

[18] J. Tan, Q. Zhao, X. Guo, X. Zhao, and G. Wang, "Radio tomographic imaging based on low-rank and sparse decomposition," *IEEE Access*, vol. 7, pp. 50223–50231, 2019.

[19] S. Xu, H. Liu, F. Gao, and Z. Wang, "Compressive sensing based radio tomographic imaging with spatial diversity," *Sensors*, vol. 19, no. 3, p. 439, Jan. 2019.

[20] A. Gonzalez-Ruiz and Y. Mostofi, "Cooperative robotic structure mapping using wireless measurements—A comparison of random and coordinated sampling patterns," *IEEE Sensors J.*, vol. 13, no. 7, pp. 2571–2580, Jul. 2013.

[21] C. R. Karanam and Y. Mostofi, "3D through-wall imaging with unmanned aerial vehicles using WiFi," in *Proc. 16th ACM/IEEE Int. Conf. Inf. Process. Sensor Netw. (IPSN)*, Apr. 2017, pp. 131–142.

[22] N. Patwari and J. Wilson, "RF sensor networks for device-free localization: Measurements, models, and algorithms," *Proc. IEEE*, vol. 98, no. 11, pp. 1961–1973, Nov. 2010.

[23] V. Estellers, J.-P. Thiran, and X. Bresson, "Enhanced compressed sensing recovery with level set normals," *IEEE Trans. Image Process.*, vol. 22, no. 7, pp. 2611–2626, Jul. 2013.

[24] W. C. Chew, *Waves and Fields in Inhomogeneous Media*. Piscataway, NJ, USA: IEEE Press, 1997, pp. 405–408.

[25] Q. Lei, H. Zhang, H. Sun, and L. Tang, "A new elliptical model for device-free localization," *Sensors*, vol. 16, no. 4, p. 577, Apr. 2016.

[26] C. Zhu and Y. Chen, "Distance attenuation-based elliptical weighting-g model in radio tomography imaging," *IEEE Access*, vol. 6, pp. 34691–34695, 2018.

[27] G. Gennarelli and F. Soldovieri, "Performance analysis of incoherent RF tomography using wireless sensor networks," *IEEE Trans. Geosci. Remote Sens.*, vol. 54, no. 5, pp. 2722–2732, May 2016.

[28] T. N. Canh, K. Q. Dinh, and B. Jeon, "Edge-preserving nonlocal weighting scheme for total variation based compressive sensing recovery," in *Proc. IEEE Int. Conf. Multimedia Expo (ICME)*, Jul. 2014, pp. 1–5.

[29] C. Li, "An efficient algorithm for total variation regularization with applications to the single pixel camera and compressive sensing," Ph.D. dissertation, Dept. Comput. Appl. Math., Rice University, Houston, TX, USA, 2010.

[30] W. Guo and W. Yin, "Edge guided reconstruction for compressive imaging," *SIAM J. Imag. Sci.*, vol. 5, no. 3, pp. 809–834, Jan. 2012.

[31] S. Boyd, "Distributed optimization and statistical learning via the alternating direction method of multipliers," *Found. Trends Mach. Learn.*, vol. 3, no. 1, pp. 1–122, 2010.

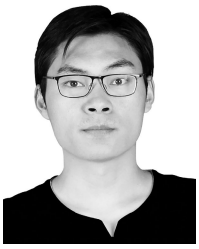

QICHANG GUO received the B.S. degree in electronic information science and technology from Jilin University, Changchun, China, in 2016. He is currently pursuing the Ph.D. degree with the National Key Lab of Microwave Imaging Technology, Chinese Academy of Sciences. His research interests include radar imaging, signal analysis, and information processing.

YANLEI LI received the Ph.D. degree from the National Key Lab of Microwave Imaging Technology, Chinese Academy of Sciences, in 2014. He has been working at the Institute of Electronics, Chinese Academy of Science, Beijing, China, since 2014. His research interests include radar imaging systems and radar signal processing.

XINGDONG LIANG received the Ph.D. degree from the Beijing Institute of Technology, Beijing, China, in 2001. He has been working at the Institute of Electronics, Chinese Academy of Science, Beijing, China, since 2002. During this period, he was responsible for many important Chinese national programs, including high-resolution synthetic aperture radar (SAR) systems. He is currently a Professor and the Deputy Director of the National Key Lab of Microwave Imaging Technology, Chinese Academy of Sciences. His research interests include radar imaging systems and radar signal processing.

JIAWEI DONG received the B.S. degree in electronic information science and technology from the Harbin Engineering University, Harbin, China, in 2018. He is currently pursuing the master's degree with the National Key Lab of Microwave Imaging Technology, Chinese Academy of Sciences. His research interests include radar imaging, moving target tracking, and information processing.

RUICHANG CHENG was born in Liaoning, China, in 1992. He received the B.Sc. degree in applied physics from the University of Science and Technology of China, in 2015. He is currently pursuing the Ph.D. degree in signal and information processing with the National Key Lab of Microwave Imaging Technology, Chinese Academy of Sciences. His researches include 3-D reconstruction of objects from point clouds and deep learning in SAR image.